crystals

MDPI

Article

Large-Scale Synthesis h-BN Films on Copper-Nickel Alloy by Atmospheric Pressure Chemical Vapor Deposition

Yuhan Feng [1], Yumin Zhang [1], Jipeng Liu [2], Ye Zhang [3,*] and Yongshuai Xie [1,*]

[1] National Key Laboratory of Science and Technology on Advanced Composites in Special Environments, Harbin Institute of Technology, Harbin 150001, China; 20sk18252@stu.hit.edu.cn (Y.F.); zhym@hit.edu.cn (Y.Z.)
[2] MIIT Key Laboratory of Critical Materials Technology for New Energy Conversion and Storage, School of Chemistry and Chemical Engineering, Harbin Institute of Technology, Harbin 150001, China; liujipeng@hit.edu.cn
[3] China Electronic Product Reliability and Environmental Testing Research Institute, Guangzhou 511370, China
* Correspondence: z18675872121@sina.com (Y.Z.); ysxie@hit.edu.cn (Y.X.)

Abstract: Due to its high thermal and chemical stability, excellent dielectric properties, unique optical properties, corrosion resistance, and oxidation resistance, the two-dimensional hexagonal boron nitride (h-BN) is often used in a thermal conductor protective layer in deep ultraviolet light-emitting detector fields. However, due to the complicated growth conditions of h-BN, it is often necessary to prepare h-BN by the CVD method in a high vacuum environment, which is limited to a certain extent in terms of film size and production cost. In order to solve this problem, we proposed a method to prepare h-BN thin films by atmospheric CVD (APCVD). This method does not need a vacuum environment, which reduces energy consumption and cost, and makes the operation simpler and the experimental environment safer. The preparation of high-quality h-BN film was carried out using a Cu-Ni alloy as the growth substrate. The growth process of h-BN film was studied, and the influence of growth parameters on the structure of the h-BN film was explored. The morphological features and elemental composition pairs of the samples were characterized and analyzed, which confirmed that the high-quality h-BN film could be successfully grown on the Cu-Ni alloy substrate by APCVD. The UV detection device prepared by using the prepared h-BN film as the photoresponse material had good photoresponse characteristics and performance stability. It provides a new idea for the low-cost preparation of large-scale h-BN.

Keywords: APCVD; h-BN; film; photoelectric devices

check for updates

Citation: Feng, Y.; Zhang, Y.; Liu, J.; Zhang, Y.; Xie, Y. Large-Scale Synthesis h-BN Films on Copper-Nickel Alloy by Atmospheric Pressure Chemical Vapor Deposition. *Crystals* **2022**, *12*, 985. https://doi.org/10.3390/cryst12070985

Academic Editor: Dah-Shyang Tsai

Received: 10 June 2022
Accepted: 12 July 2022
Published: 15 July 2022

Publisher's Note: MDPI stays neutral with regard to jurisdictional claims in published maps and institutional affiliations.

Copyright: © 2022 by the authors. Licensee MDPI, Basel, Switzerland. This article is an open access article distributed under the terms and conditions of the Creative Commons Attribution (CC BY) license (https://creativecommons.org/licenses/by/4.0/).

1. Introduction

Two-dimensional hexagonal boron nitride (h-BN) has excellent thermal stability, good thermal conductivity and electrical insulation, unique ultraviolet light emission, high mechanical strength, and dielectric properties, and is widely used in optoelectronic devices, dielectric materials, multifunctional coating materials, and self-cleaning devices [1–5]. In addition, h-BN has an atomically smooth surface without dangling bonds or charge traps and thus is considered an ideal substrate for electronic devices based on other 2D materials such as graphene and transition metal dichalcogenides (TMDs) [6–8]. Among the many preparation methods for h-BN thin films, the chemical vapor deposition (CVD) method is the most commonly used due to its better controllability. In particular, it provides a solution for the preparation of large-area, high-quality BN thin films, which is very important for practical applications. At present, many researchers have focused on the preparation of high-quality h-BN thin films by CVD technology, and high-quality h-BN thin films have been obtained using different raw materials [9–12]. However, most of the films reported have been fabricated in a low-pressure vacuum environment [13–15]. Complex preparation conditions greatly limit its further development and application. Excitingly, Shi et al. [16] prepared few-layer h-BN thin films on metallic nickel in an atmospheric pressure CVD

(APCVD) system using ammonia borane as the raw material. The film thickness was 5 nm to 50 nm but its size was limited by the nickel grains. How to use the APCVD method to obtain larger sized h-BN thin films is the key to its further application and development, and it is also the bottleneck faced by the current industry.

As a protective film or insulating film, a continuous h-BN film with a certain thickness is essential. So far, multilayer h-BN continuous layers have been fabricated on various transition metal substrates such as Cu [17,18], Ni [16,19,20], Pt [21], and Co [22] by the CVD method. However, the morphology of the metal substrate has an impact on the nucleation and growth of h-BN thin films, and most of the gas molecules are first adsorbed on the roughness of the metal surface or impurity sites during the growth process due to the influence of the gas flow. In order to solve this problem, researchers have made many efforts. Lee et al. [23] studied the influence of the surface morphology of copper foil on the growth of h-BN. By electrochemically polishing the surface of the copper foil, a flatter surface of the copper foil was obtained, which resulted in increased surface grain boundaries and roughness. The surface of the copper foil with a reduced grain boundary was prepared, the h-BN film with less grain boundary surfaces was prepared, and it was applied to the field-effect transistor device of graphene, which improved the electrical properties of graphene. Tay et al. [24] first performed electrochemical polishing on the surface of the copper foil to make the surface cleaner and smoother than the surface before annealing, which greatly eliminated the roughness of the copper surface and increased the grain boundaries of the surface. The h-BN monoliths and continuous films with hexagonal morphology were obtained, and the area of the monolith reached 35 μm^2. In addition to using a single metal as the substrate to prepare h-BN, Lu et al. [25] reported the preparation of regular triangular shaped h-BN monoliths with a maximum size of 100 μm using a Cu-Ni alloy as a substrate. At the same time, it was used as a dielectric layer in graphene field-effect transistor devices to improve the electrical properties of graphene. Caneva et al. [26] used a Si-assisted method to prepare h-BN monolithic and continuous films with jagged edges and a triangular shape of 300 μm on iron metal substrates. Zhang et al. [27] used the Ni/(B, N)/Fe growth system to synthesize h-BN thin films by the co-segregation method. By adjusting the thickness of the Fe film and (B, N), the growth mode could be adjusted during the growth process to obtain the sub-monolayer, single-layer h-BN and multilayer h-BN with various thicknesses. Yang et al. [28] reported 2D h-BN single domains on a Cu/Ni alloy via the APCVD method, and the shape of h-BN could be adjusted by the Ni content of the Cu/Ni substrate.

In this work, we employed the APCVD method with a Cu-Ni alloy as the growth substrate to explore the effect of growth process parameters on the structure of h-BN thin films and realize the controllable preparation of high-quality h-BN thin films. On this basis, an ultraviolet detection device was developed and its performance was evaluated.

2. Materials and Methods

2.1. Materials

Copper foil (Taizhou Sunano New Energy Co., Ltd., Taizhou, China), ethanol (C_2H_5OH, AR, Damao Chemical Reagent Factory, Tianjin, China), acetone (CH_3COCH_3, AR, Damao Chemical Reagent Factory, Tianjin, China), HCl, polyethylene glycol (Shanghai Aladdin Biochemical Technology Co., Ltd., Shanghai, China), phosphoric acid (Shanghai Aladdin Biochemical Technology Co., Ltd., Shanghai, China), $NiSO_4 \cdot 6H_2O$ (Shanghai Aladdin Biochemical Technology Co., Ltd., Shanghai, China), $NiCl_2 \cdot 6H_2O$ (Shanghai Aladdin Biochemical Technology Co., Ltd., Shanghai, China), NaF (Shanghai Aladdin Biochemical Technology Co., Ltd., Shanghai, China), H_3BO_3 (Shanghai Aladdin Biochemical Technology Co., Ltd., Shanghai, China), Borane ammine complex (Shanghai Aladdin Biochemical Technology Co., Ltd., Shanghai, China), and deionized water were used as starting materials in this study. All chemicals were used as starting materials without further purification.

2.2. Methods

Using copper foil (Figure 1a) and the Cu-Ni alloy as the growth substrate of hexagonal boron nitride, the experimental process included the following steps:

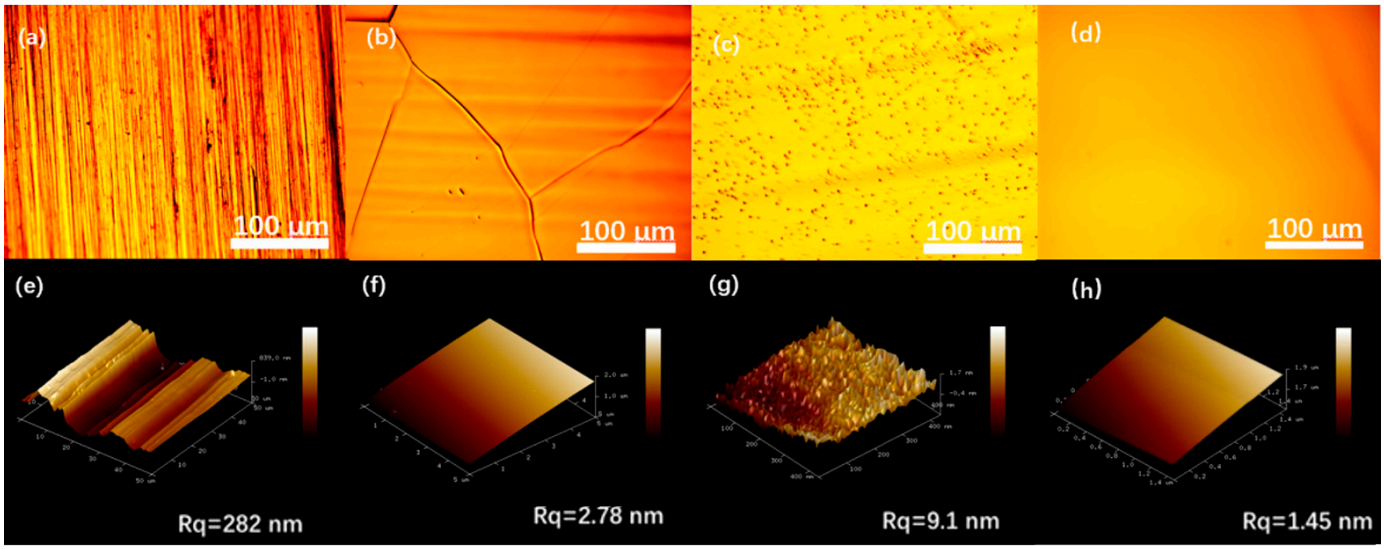


Figure 1. Optical microscopy images of (**a**) untreated substrate, (**b**) cleaned and polished annealed substrate, (**c**) nickel-plated substrate, and (**d**) re-annealing to synthesize copper-nickel alloys. 3D atomic force microscopy height images of (**e**) untreated substrate, (**f**) cleaned and polished annealed substrate, (**g**) nickel-plated substrate, and (**h**) re-annealing to synthesize copper-nickel alloys.

(1) Pretreatment of metal: The pretreatment of metal foil included cleaning and polishing. When cleaning, the metal foil needed to be sonicated in deionized water for 10 min, ethanol for 10 min, and acetone for 10 min to remove impurities and attachments on the surface. We performed subsequent sonication in 25% HCl solution for 10 min to remove the oxide layer on the surface. Finally, we rinsed continuously with deionized water and blew dry with N_2. When polishing, the metal foil needed to be placed in a polishing solution composed of a solution of polyethylene glycol: 85% phosphoric acid = 1:3. The metal foil was connected to the power supply cathode and polished in constant voltage mode. The polishing voltage was set between 1.2 V and 1.8 V, and the polishing time was determined by the specific polishing brightness. We rinsed with copious amounts of deionized water after polishing and dried with N_2. We heated to 1070 °C in a tube furnace for 5–8 h for annealing, and Figure 1b exhibits the cleaning and polishing of the annealed substrate.

(2) Preparation of the Cu-Ni alloy: The copper foil with a thickness of 50 μm was used as the substrate, and the surface was electrochemically plated with nickel by the electrochemical method. The electrolyte consisted of 250 mL H_2O, 70 g $NiSO_4 \cdot 6H_2O$, 2 g $NiCl_2 \cdot 6H_2O$, 1 g NaF, and 7.5 g H_3BO_3. A constant current of 0.01 A was used. By changing the deposition time, the thickness of the Ni layer could be changed. After the deposition process, we rinsed with copious amounts of deionized water and blew dry with N_2, and the substrate after nickel plating is shown in Figure 1c. It was placed in a tube furnace, heated to 1060–1075 °C, and maintained for 4–8 h to form a uniform Cu-Ni alloy (Figure 1d).

(3) Growth h-BN on the surface of the Cu-Ni alloy: h-BN was prepared by the atmospheric pressure chemical vapor deposition method with a Cu-Ni alloy as the growth substrate. Borane ammine complex (10 mg, 55 cm from the metal substrate) was used as the precursor for the reaction, and it was heated to 102–105 °C to decompose to produce active particles with 120 sccm Ar and 20 sccm H_2 as the reaction atmosphere. The metal surface in the center of the furnace's temperature adsorbed, migrated, nucleated, and expanded continuously to generate hexagonal boron nitride at 1070 °C. The growth time was controlled between 5–60 min. We moved the raw material to the low-temperature area,

which makes the hexagonal boron nitride stop growing, and at the same time, we reduced the furnace temperature and waited until it dropped to room temperature.

The surface roughness of the substrates obtained by different treatment methods are shown in Figure 1e–h. The surface roughness of substrates under different treatments is shown in Table 1.

Table 1. The surface roughness of substrates under different treatments.

	Untreated Substrate	Cleaned and Polished Annealed Substrate	Nickel-Plated Substrate	Re-Annealing to Synthesize Copper-Nickel Alloys
Surface roughness	282 nm	2.78 nm	9.1 nm	1.45 nm

2.3. Transfer

The hexagonal boron nitride prepared on the copper-nickel substrate needed to be transferred to the SiO_2/Si substrate. We used the PMMA-assisted method to transfer it to the SiO_2/Si substrate. First, we spin-coated a layer of PMMA on the surface of the copper-nickel substrate grown with hexagonal boron nitride and dried it on a hot stage at 150 °C for 10–30 min. Then, using KOH solution as the solution, copper-nickel substrate as the negative electrode, metal platinum as the positive electrode, and using a 2.7 V DC power supply, the PMMA-coated hexagonal boron nitride was peeled off by generating hydrogen bubbling at the negative electrode and then transferred. In deionized water, it was repeatedly washed several times, and then we used the SiO_2/Si substrate to pick up the film. After removing moisture in an oven, we removed PMMA with acetone solution. At this point, our thin film of hexagonal boron nitride was transferred to the target substrate.

2.4. Characterization

The microscopic morphology of the samples was characterized by an optical microscope (Olympus BX53M, Tokyo, Japan) and a scanning electron microscope (SEM, Hitachi S-4800, Tokyo, Japan), and the distribution of elements in the prepared copper-nickel alloy substrate was analyzed by an energy dispersive spectrometer equipped (EDS, Oxford Instruments, Bognor Regis, UK) with SEM. Since h-BN does not have any contrast on the surface of the metal substrate, it is not easy to observe directly by an optical microscope (OM). Here, we applied the characterization of the antioxidant properties of h-BN. The metal substrate after the growth of h-BN was oxidized in the air. Since the area covered by h-BN is not easily oxidized, the area not covered by h-BN is directly oxidized, which could well display the microstructure of h-BN. To enhance the optical contrast of metal substrate samples under an optical microscope, they are generally oxidized in air at 200 °C for 5 min before observation. The surface chemical properties of the samples were analyzed by X-ray photoelectron spectroscopy (XPS, ESCALAB 250 Thermo Fisher SCIENTIFIC, Waltham, MA, USA), and the test results were calibrated with C 1s (284.8 eV). In addition, the h-BN film was analyzed by a Raman spectrometer (Raman, LabRAM HR 800, Jobin Yvon, France), and the wavelength used for the test was 532 nm.

3. Results and Discussion

For Cu-Ni alloys, due to the similar atomic structures of the two, the difference in the atomic radii is small. Nickel atoms can penetrate the lattice of copper atoms to occupy the junction positions of copper atoms. The solute atom Ni can replace part of the lattice of the solvent atom Cu, and the crystal structure of the new substance remains the same as that of the solvent atom, forming a Cu-Ni solid solution. The higher temperature ensures that the diffusion is fully carried out and the internal element distribution is uniform. The Cu foils were first cleaned, polished, annealed, nickel-plated, and re-annealed, which could increase the surface flatness and the average size of the grains. Figure 2 shows the SEM images of the surface morphology and cross-sectional morphology of the Cu-Ni alloy after plating for

30 min and high-temperature treatment, as well as the energy spectrum scanning images of the corresponding area. From the cross-sectional view, the nickel layer plated on the surface of the copper foil was uniformly diffused into the copper foil to form a uniform Cu-Ni alloy (Figure 2a–c). One could see from Figure 2d that the surface of the Cu-Ni alloy was very uniform and there was no obvious crystal nucleus precipitation. Ni atoms diffused uniformly on the surface of the Cu foil and penetrated the interior, indicating the formation of a uniform Cu-Ni alloy (Figure 2e,f). There is no doubt that further prolonging the electroplating time could increase the quality of the Ni layer deposited on the surface of the copper foil and the content of Ni in the alloy. In addition, combined with an energy dispersive X-ray spectroscopy (EDS), the composition ratio of copper and nickel atoms in the Cu-Ni alloy was obtained (Table 2). We analyzed the quality of the metal foil before and after the electroplating experiment and before and after the annealing treatment by analytical balance. The quality change was calculated and the content of Ni in the Cu-Ni alloy was calculated to be 5%, which was consistent with the alloy ratio measured by EDS.

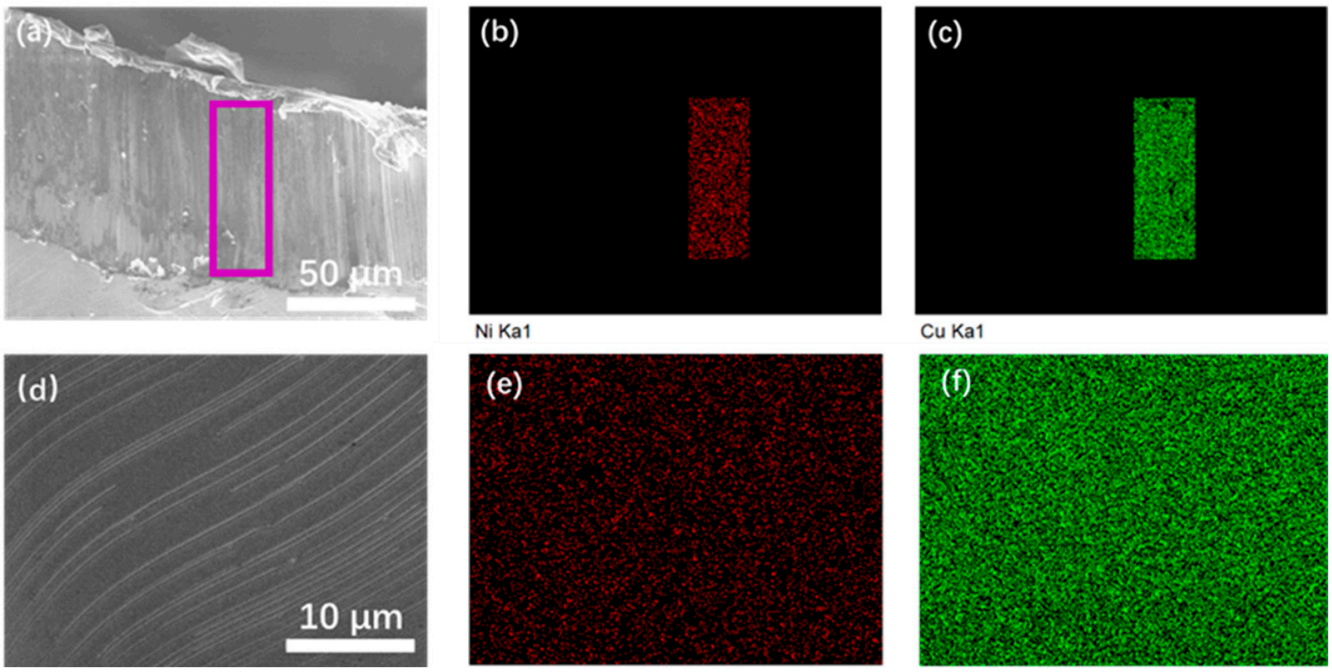


Figure 2. (**a**) SEM image of the cross-section and (**b**,**c**) corresponding EDS mappings of Cu and Ni elements, respectively, (**d**) SEM image of the surface and (**e**,**f**) corresponding EDS mappings of Cu and Ni elements, respectively.

Table 2. Metal content in different regions of Cu-Ni alloys.

Elements	Surface	Cross-Section
Ni (%)	5.30	5.29
Cu (%)	94.70	94.71
Total (%)	100.00	100.00

The growth trend and morphology change of h-BN by heating and oxidizing the grown substrate in the air with the prolongation of the reaction time are shown in Figures 3 and 4. Within 1 min of the reaction, h-BN did not start growing on the substrate (Figure 3a). Over time, h-BN gradually started to deposit on the substrate. When the reaction was performed for 5 min, the hexagon grown h-BN on the substrate could be clearly seen (Figure 3b). After 10 min of reaction, the h-BN on the substrate was connected to form a film, which completely covered the surface of the substrate to form a few-layer structure. In the subsequent process, with the continuous deposition of h-BN, the number and thickness

of h-BN layers continued to increase. The multi-layer film structure could be clearly seen when the reaction time reached 11 min, and the multi-layer structure became more obvious with the prolongation of the reaction time. It is worth noting that the size of the as-obtained h-BN film was in the order of hundreds of microns, and the area was much larger than that of the h-BN film prepared by the APCVD method reported previously [16]. In order to further study the structural characteristics of the h-BN film and its application performance as an ultraviolet optoelectronic device, the samples obtained by the reaction for 10 min were selected to carry out follow-up research work.

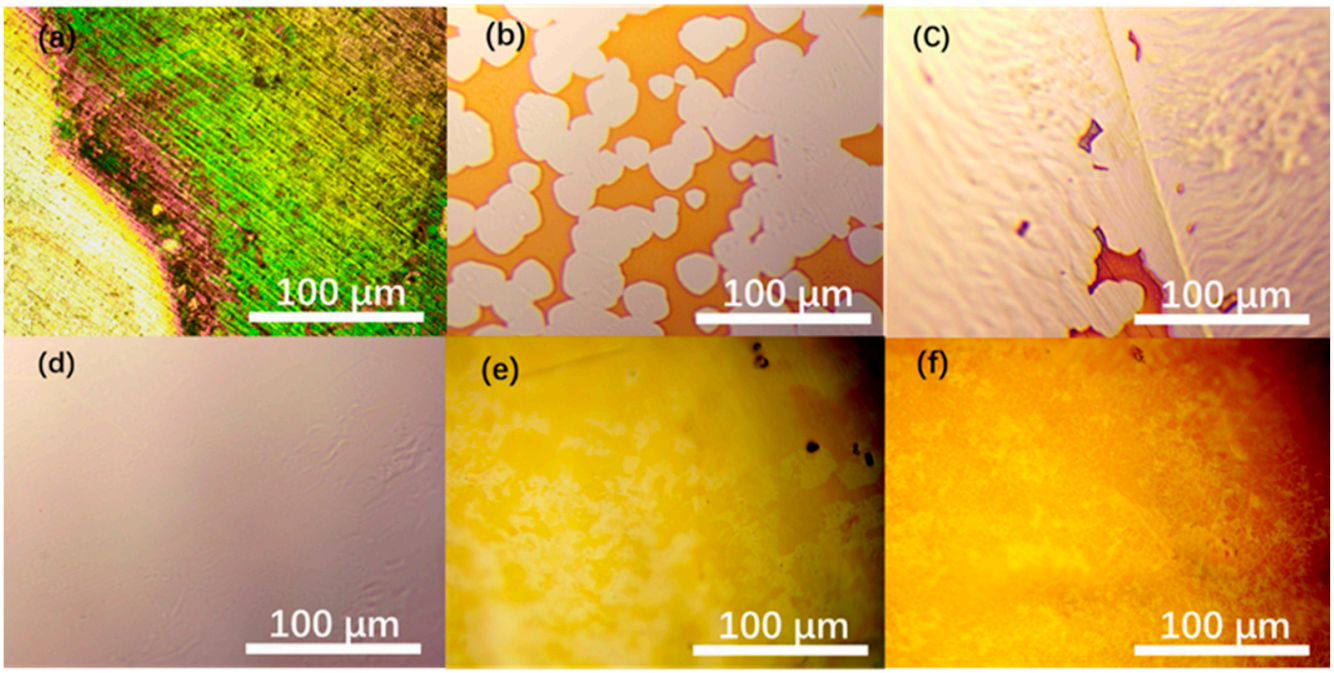


Figure 3. Growth states of h-BN on substrates with different reaction times. (**a**) 1 min, (**b**) 5 min, (**c**) 7 min, (**d**) 10 min, (**e**) 11 min, and (**f**) 15 min.

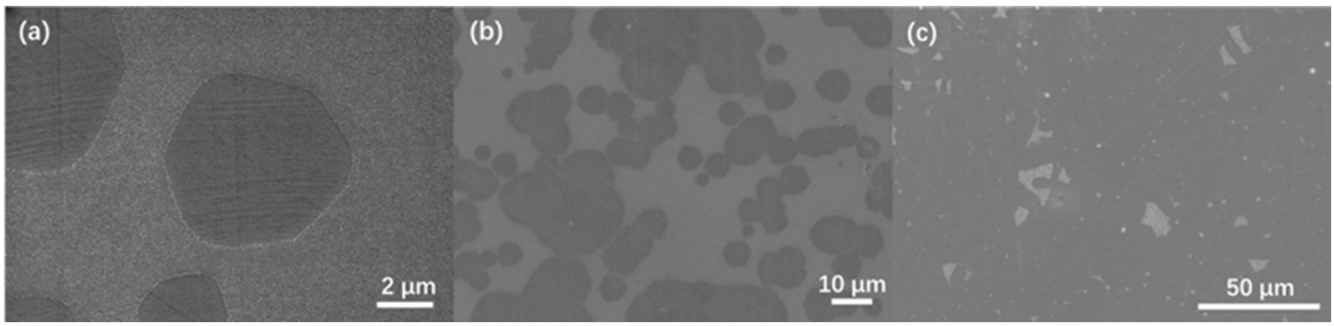


Figure 4. The SEM results of different reaction times h-BN on substrates. (**a**) 3 min, (**b**) 5 min, and (**c**) 7 min.

The roughness of an h-BN single crystal was Rq = 2.66 nm, and the roughness of an h-BN thin film was Rq = 1.86 nm (Figure 5). The thickness of the h-BN film prepared after 11 min of growth was 2.66 nm by atomic force microscopy observation of the step between the film and the substrate, and the thickness of the h-BN film prepared after 15 min of growth was 7.10 nm, as shown in Figure 6.

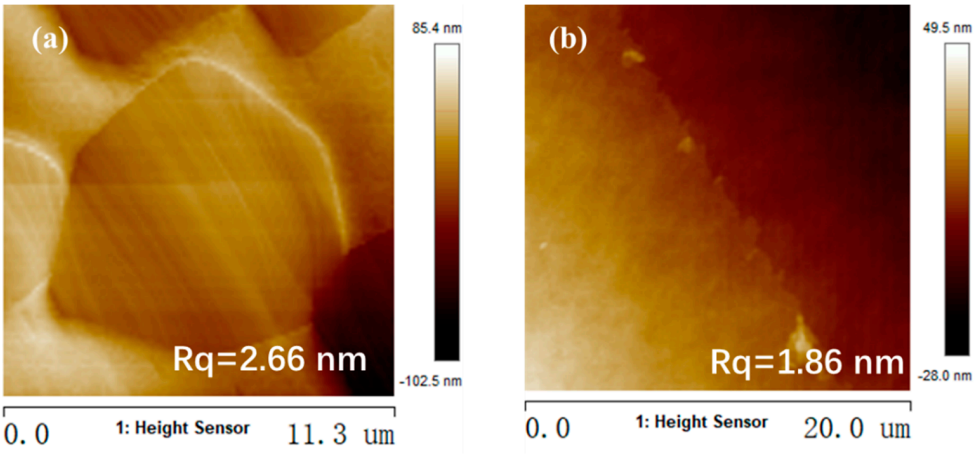


Figure 5. The surface roughness of grown h-BN. (**a**) The roughness of h-BN single crystal, (**b**) the roughness of h-BN thin film.

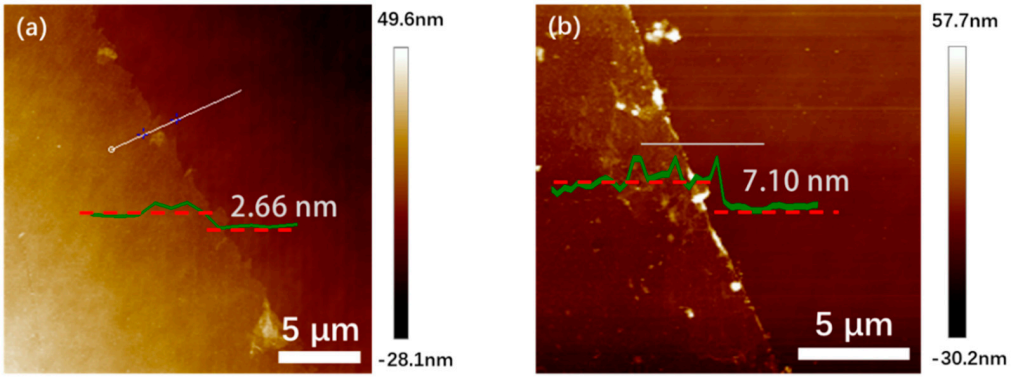


Figure 6. The film thickness of h-BN on substrates with different reaction times. (**a**) 11 min, (**b**) 15 min.

The surface chemical properties of the samples were analyzed by XPS, and the results were corrected with C 1s (284.8 eV). The XPS peaks at 190.63 eV and 398.18 eV were attributed to B 1s and N 1s in the B-N bond (Figure 7), respectively, which are consistent with the XPS of h-BN reported in the literature [7], indicating that h-BN films were successfully obtained. In addition, the as-obtained h-BN film was further analyzed using Raman spectroscopy (Figure 8). In order to avoid the influence of the substrate on the test results, we chose to transfer the h-BN film from the Cu-Ni alloy substrate to the SiO_2/Si surface for testing and use SiO_2/Si as the control. Compared with SiO_2/Si (Figure 5b), Figure 5a shows an obvious characteristic Raman peak of h-BN E_{2g} at 1369 cm^{-1}. It was further proved that we obtained an h-BN film by the APCVD mothed.

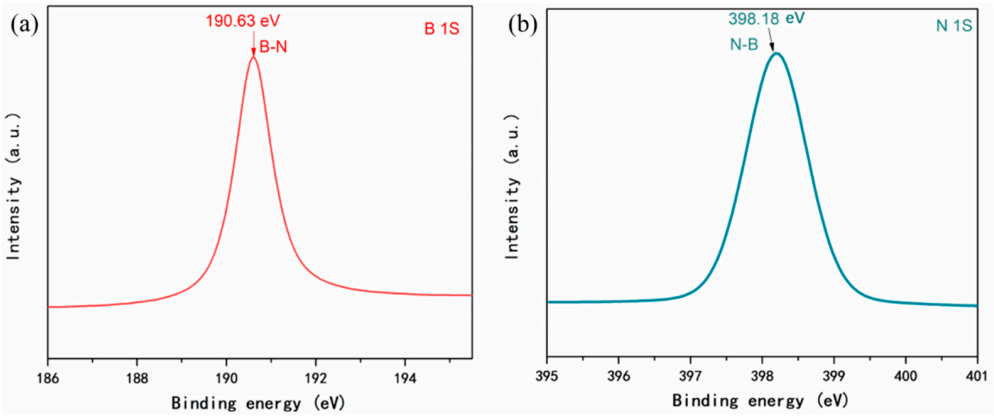


Figure 7. XPS peaks of h-BN. (**a**) B 1s, (**b**) N 1s.

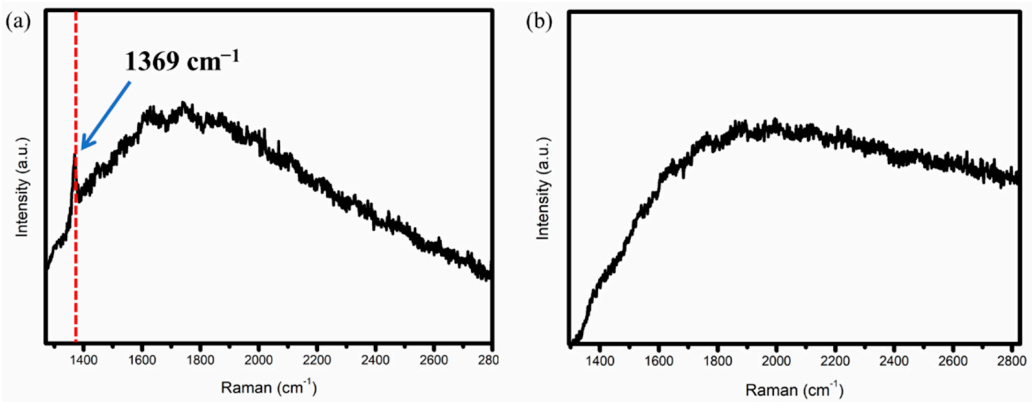


Figure 8. (**a**) Raman peaks transferred from h-BN grown on Ni-containing 5% Cu-Ni alloy substrates to SiO_2/Si, (**b**) Raman peak of SiO_2/Si.

In order to study the application performance of h-BN as a UV photodetector, we used the obtained h-BN film as the channel material and fabricated UV detection photoelectric devices via the mask method and metal deposition method. Figure 9 shows the schematic and optical microscope images of the device. When fabricating the device, firstly, the h-BN film grown on the Cu-Ni alloy containing 5% Ni was transferred to the SiO_2/Si surface under the optical microscope to construct the device. Then, the h-BN film was masked and only the two ends were left outside. Finally, 25 nm Au electrodes were deposited on the exposed areas at both ends using a thermal evaporation coater to form metal electrodes to obtain ultraviolet optoelectronic devices.

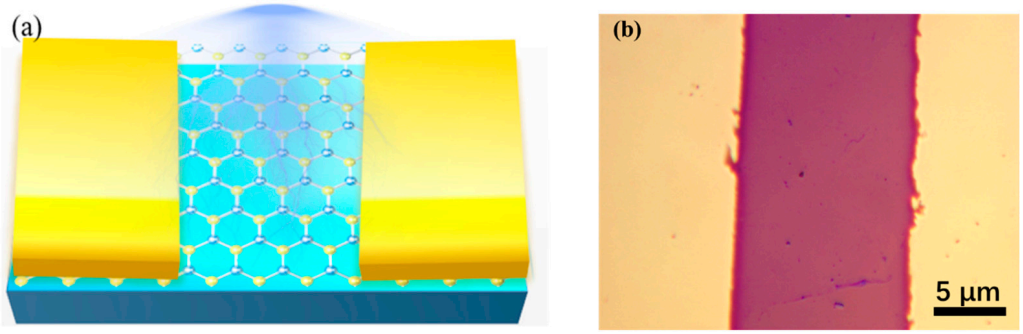


Figure 9. (**a**) Schematic and (**b**) optical image of the device.

The photoelectric response performance of the device was tested by a temperature-variable probe analysis station (Lakeshore) and semiconductor tester (4200-SCS). We used a DD2.5TZ deuterium lamp as the UV light source, the power of which was 30 W. The photoresponse characteristic and stability of UV detectors were studied by cycling on-off the UV light source (Figure 10). When the UV light source was turned on, the number of charge carriers increased immediately, resulting in a dramatic increase in the photocurrent observed at the left edge of each current pulse. When the light source was turned off, the photocurrent dropped to the starting position. Repeatedly turning on-off the UV light source showed little deviation in the photocurrent intensity and duration period, indicating that the photoresponse of our device was reversible and stable.

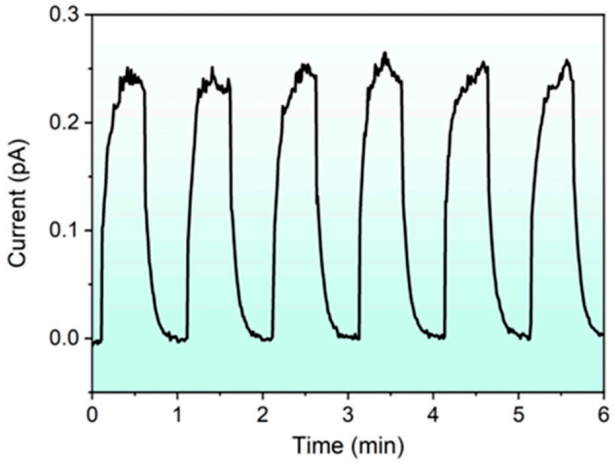


Figure 10. Photoresponse characteristic and stability of the device.

4. Conclusions

In this work, a Cu-Ni alloy was used as the substrate, and the h-BN film was prepared by the APCVD method. The size of the h-BN film was in the order of hundreds of microns, which was much larger than the existing reported results via the same method. The structure of the film could be controlled by adjusting the reaction time, and the film obtained by reacting for 10 min could uniformly cover the surface of the substrate to form a few-layer structure. The UV detection device prepared by using the as-obtained h-BN film as a UV-responsive substance had excellent photoresponse performance and good performance stability and has certain application prospects in the field of UV photodetection.

Author Contributions: Conceptualization, Y.Z. (Yumin Zhang); investigation, Y.F., J.L., Y.Z. (Ye Zhang); writing—original draft preparation, Y.F.; writing—review and editing, Y.Z. (Yumin Zhang), Y.X.; supervision, Y.F.; project administration, Y.Z. (Yumin Zhang); funding acquisition, Y.X. All authors have read and agreed to the published version of the manuscript.

Funding: This research was funded by Heilongjiang Provincial Postdoctoral Science Foundation, grant number LBH-Z21050.

Institutional Review Board Statement: Not applicable.

Informed Consent Statement: Not applicable.

Data Availability Statement: Not applicable.

Conflicts of Interest: The authors declare no conflict of interest.

References

1. Pakdel, A.; Bando, Y.; Golberg, D. Nano boron nitride flatland. *Chem. Soc. Rev.* **2014**, *43*, 934–959. [CrossRef] [PubMed]
2. Liu, H.; Meng, J.; Zhang, X.; Chen, Y.; Yin, Z.; Wang, D.; Wang, Y.; You, J.; Gao, M.; Jin, P. High-performance deep ultraviolet photodetectors based on few-layer hexagonal boron nitride. *Nanoscale* **2018**, *10*, 5559–5565. [CrossRef] [PubMed]
3. Zhi, C.; Bando, Y.; Tang, C.; Kuwahara, H.; Golberg, D. Large-scale fabrication of boron nitride nanosheets and their utilization in polymeric composites with improved thermal and mechanical properties. *Adv. Mater.* **2009**, *21*, 2889–2893. [CrossRef]
4. Liu, Z.; Gong, Y.; Zhou, W.; Ma, L.; Yu, J.; Idrobo, J.C.; Jung, J.; MacDonald, A.H.; Vajtai, R.; Lou, J.; et al. Ultrathin high-temperature oxidation-resistant coatings of hexagonal boron nitride. *Nat. Commun.* **2013**, *4*, 2541. [CrossRef]
5. Chilkoor, G.; Karanam, S.P.; Star, S.; Shrestha, N.; Sani, R.K.; Upadhyayula, V.K.K.; Ghoshal, D.; Koratkar, N.A.; Meyyappan, M.; Gadhamshetty, V. Hexagonal boron nitride: The thinnest insulating barrier to microbial corrosion. *ACS Nano* **2018**, *12*, 2242–2252. [CrossRef]
6. Dean, C.R.; Young, A.F.; Meric, I.; Lee, C.; Wang, L.; Sorgenfrei, S.; Watanabe, K.; Taniguchi, T.; Kim, P.; Shepard, K.L.; et al. Boron nitride substrates for high-quality graphene electronics. *Nat. Nanotechnol.* **2010**, *5*, 722–726. [CrossRef]
7. Joo, M.K.; Moon, B.H.; Ji, H.; Han, G.H.; Kim, H.; Lee, G.; Lim, S.C.; Suh, D.; Lee, Y.H. Electron excess doping and effective schottky barrier reduction on the MoS_2/h-BN heterostructure. *Nano Lett.* **2016**, *16*, 6383–6389. [CrossRef]
8. Kim, S.M.; Hsu, A.; Park, M.H.; Chae, S.H.; Yun, S.J.; Lee, J.S.; Cho, D.H.; Fang, W.; Lee, C.; Palacios, T.; et al. Synthesis of large-area multilayer hexagonal boron nitride for high material performance. *Nat. Commun.* **2015**, *6*, 8662. [CrossRef]

9. Rozenberg, A.S.; Sinenko, Y.A.; Chukanov, N.V. Regularities of pyrolytic boron coating formation on graphite matrix. *J. Mater. Sci.* **1993**, *28*, 5528–5533. [CrossRef]
10. Middleman, S. The role of gas-phase reaction in boron nitride growth by chemical vapor deposition. *Mater. Sci. Eng.* **1993**, *63*, 135–140. [CrossRef]
11. Adams, A.C. Characterization of film formed by pyrolysis of borazine. *J. Electrochem. Soc.* **1981**, *128*, 1378–1379. [CrossRef]
12. Pierson, H.O. Boron nitride composites by chemical vapor deposition. *J. Compos. Mater.* **1975**, *9*, 228–240. [CrossRef]
13. Chen, T.A.; Chuu, C.P.; Tseng, C.C.; Wen, C.K.; Wong, H.S.P.; Pan, S.; Li, R.; Chao, T.A.; Chueh, W.C.; Zhang, Y.; et al. Wafer-scale single-crystal hexagonal boron nitride monolayers on Cu(111). *Nature* **2020**, *579*, 219–223.
14. Aldalbahi, A.; Li, E.; Rivera, M.; Velazquez, R.; Altalhi, T.; Peng, X.; Feng, P.X. Structural and electronic properties of epitaxial multilayer h-BN on Ni(111) for spintron-ics applications. *Sci. Rep.* **2016**, *6*, 23457. [CrossRef] [PubMed]
15. Gorbachev, R.V.; Riaz, I.; Nair, R.R.; Jalil, R.; Britnell, L.; Belle, B.D.; Hill, E.W.; Novoselov, K.S.; Watanabe, K.; Taniguchi, T.; et al. Hunting for monolayer boron nitride: Optical and Raman signatures. *Small* **2011**, *7*, 465–468. [CrossRef] [PubMed]
16. Shi, Y.M.; Hamsen, C.; Jia, X.T.; Kim, K.K.; Reina, A.; Hofmann, M.; Hsu, A.L.; Zhang, K.; Li, H.N.; Juang, Z.Y.; et al. Synthesis of few-layer hexagonal boron nitride thin film by chemical vapor deposition. *Nano Lett.* **2010**, *10*, 4134–4139. [CrossRef] [PubMed]
17. Song, L.; Ci, L.; Lu, H.; Sorokin, P.B.; Jin, C.; Ni, J.; Kvashnin, A.G.; Kvashnin, D.G.; Lou, J.; Yakobson, B.I.; et al. Large scale growth and characterization of atomic hexagonal boron nitride layers. *Nano Lett.* **2010**, *10*, 3209–3215. [CrossRef]
18. Tay, R.Y.; Wang, X.; Tsang, S.H.; Loh, G.C.; Singh, R.S.; Li, H.; Mallick, G.; Teo, E.H.T.A. systematic study of the atmospheric pressure growth of large-area hexagonal crystalline boron nitride film. *J. Mater. Chem. C* **2014**, *2*, 1650–1657. [CrossRef]
19. Ismach, A.; Chou, H.; Ferrer, D.A.; Wu, Y.; McDonnell, S.; Floresca, H.C.; Covacevich, A.; Pope, C.; Piner, R.; Kim, M.J.; et al. Toward the controlled synthesis of hexagonal boron nitride films. *ACS Nano* **2012**, *6*, 6378–6385. [CrossRef]
20. Lee, Y.H.; Liu, K.K.; Lu, A.Y.; Wu, C.Y.; Lin, C.T.; Zhang, W.; Su, C.Y.; Hsu, C.L.; Lin, T.W.; Wei, K.H.; et al. Growth selectivity of hexagonal-boron nitride layers on Ni with various crystal orientations. *RSC Adv.* **2012**, *2*, 111–115. [CrossRef]
21. Gao, Y.; Ren, W.; Ma, T.; Liu, Z.; Zhang, Y.; Liu, W.; Ma, L.; Ma, X.; Cheng, H. Repeated and controlled growth of monolayer, bilayer and few-layer hexagonal boron nitride on Pt foils. *ACS Nano* **2013**, *7*, 5199–5206. [CrossRef] [PubMed]
22. Orofeo, C.M.; Suzuki, S.; Kageshima, H.; Hibino, H. Growth and low-energy electron microscopy characterization of monolayer hexagonal boron nitride on epitaxial cobalt. *Nano Res.* **2013**, *6*, 335–347. [CrossRef]
23. Lee, K.H.; Shin, H.J.; Lee, J.; Lee, I.; Kim, G.H.; Cho, J.Y.; Kim, S.W. Large-Scale Synthesis of High-Quality Hexagonal Boron Nitride Nanosheets for Large-Area rapheme Electronic. *Nano Lett.* **2012**, *12*, 714–718. [CrossRef] [PubMed]
24. Tay, R.Y.; Griep, M.H.; Mallick, G.; Tsang, S.H.; Singh, R.S.; Tumlin, T.; Teo, E.H.T.; Karna, S.P. Growth of Large Single-Crystalline Two-Dimensional Boron Nitride Hexagons on Electropolished Copper. *Nano Lett.* **2014**, *14*, 839–846. [CrossRef]
25. Lu, G.Y.; Wu, T.R.; Yuan, Q.H.; Wang, H.S.; Wang, H.M.; Ding, F.; Xie, X.M.; Jiang, M.H. Synthesis of Large Single-Crystal Hexagonal BoronNitride Grains on Cu-Ni Alloy. *Nat. Commun.* **2015**, *6*, 6160–6167. [CrossRef]
26. Caeva, S.; Wwatherup, R.S.; Bayer, B.C.; Brennan, B.; Spencer, S.J.; Mingard, K.; Cabrero-Vilatela, A.; Baehtz, C.; Pollard, A.J.; Hofmann, S. Nucleation Control for Large, Single Crystalline Domains of Monolayer Hexagonal Boron Nitride via Si-Doped Fe Catalysts. *Nano Lett.* **2015**, *15*, 1867–1875.
27. Zhang, C.H.; Fu, L.; Zhao, L.S.; Zhou, Y.; Peng, L.H.; Liu, Z.F. Controllable Co-Segregation Synthesis of Wafer-Scale Hexagonal Boron Nitride Thin Films. *Adv. Mater.* **2014**, *26*, 1776–1781. [CrossRef]
28. Yang, H.H.; Fu, L.; Wang, L.F.; Zhou, Y.; Cao, F.; Dai, M.H.; Hu, Y.X.; Chen, H.Y.; Zhang, J.; Qiu, Y.H.; et al. Shape evolution of two dimensional hexagonal boron nitride single domains on Cu/Ni alloy and its applications in ultraviolet detection. *Nanotechnology* **2019**, *30*, 245706. [CrossRef]